Local Moment Formation in Quantum Point Contacts

Kenji Hirose,[1] Yigal Meir,[2,3,*] and Ned S. Wingreen[2]

[1]*Fundamental Research Laboratories, NEC Corporation, 34 Miyukigaoka, Tsukuba, Ibaraki 305-8501, Japan*
[2]*NEC Research Institute, 4 Independence Way, Princeton, New Jersey 08540*
[3]*Physics Department, Princeton University, Princeton, New Jersey 08540*

(Received 30 July 2002; published 17 January 2003)

Spin-density-functional theory of quantum point contacts (QPCs) reveals the formation of a local moment with a net of one electron spin in the vicinity of the point contact—supporting the recent report of a Kondo effect in a QPC. The hybridization of the local moment to the leads decreases as the QPC becomes longer, while the on site Coulomb-interaction energy remains almost constant.

DOI: 10.1103/PhysRevLett.90.026804 PACS numbers: 73.61.–r, 71.15.Mb, 71.70.Ej

The discovery of the extra conductance plateaus at $0.7(2e^2/h)$ in quantum point contacts (QPCs) [1–3] and at $0.5(2e^2/h)$ in clean quantum wires [4], in addition to the usual quantization of the conductance into steps of $2e^2/h$ [5,6], has focused attention on the role of electron-electron interaction in these low-dimensional quantum systems [7–12].

A recent experiment on QPCs has revealed several features characteristic of the Kondo effect [13]. Specifically, there is a zero-bias peak in the differential conductance which splits in an in-plane magnetic field [14]. A single energy scale, the "Kondo" temperature T_K, sets the width of the zero-bias peak, the magnetic field required to split the peak, and the crossover temperature to perfect transmission. Moreover, the extra conductance plateau at $0.7(2e^2/h)$ can be explained using an Anderson model in which the hybridization of a localized electron to the band depends on energy and valence [15]. A puzzling question is how a localized spin can form in an open QPC system.

In this work, we employ spin-density-functional theory (SDFT) and find that a local moment with a net of one electron spin is formed in the vicinity of a QPC. The splitting between the two spin directions at high in-plane magnetic fields [14] approaches a finite residual splitting at zero field, which we interpret as the Coulomb-interaction energy U between electrons at the site of the QPC. From the width of the localized state, we infer that the hybridization to the leads decreases for longer QPCs, while the Coulomb U remains nearly constant. Our interpretation that a *dynamical* local moment forms at the QPC differs from that of Wang and Berggren [7], who infer a true spin-polarized ground state. We believe that the experimental observation of signatures of the Kondo effect [13], combined with a theorem forbidding spin polarization in one dimension [16], strongly favor the dynamical-spin interpretation.

The electronic states of a realistic quantum point contact are obtained using density-functional theory within the local-density approximation [17]. This method allows us to study both potential confinement and electron-electron interaction in a unified framework. First, for a clean quantum wire uniform in the x direction and with a parabolic confining potential in the y direction of $V^0_{\rm ext}(y) = (1/2)m^*\omega_y^2 y^2$, we readily find the wave functions $e^{\pm ik_n^\sigma x}\psi_n^\sigma(y)$, chemical potential μ, band-edge energies ϵ_n^σ, and the charge density $\rho^{0\sigma}(y)$ for a given density $n_{\rm 1D}$ [18]. Here n is the subband index and σ is the spin index, respectively.

Next, we introduce the QPC potential,

$$V_{\rm QPC}(x, y) = V(x)/2 + m^*[\omega_y + V(x)/\hbar]^2 y^2/2 - V^0_{\rm ext}(y), \tag{1}$$

(see insets in Fig. 1), where $V(x) = V_0/\cosh^2(x/d)$, with decay length $d = \sqrt{2V_0/m^*}/\omega_x$, and solve the following Kohn-Sham equation [19] for wave functions with energy ϵ,

$$\left[-\frac{\hbar^2}{2m^*}\frac{\partial^2}{\partial x^2} + V_{\rm QPC}(x, y) + \delta V_H(x, y) + \delta V^\sigma_{\rm xc}(x, y) + g\mu_B B_\parallel \sigma + \epsilon_n^\sigma\right]\Psi^\sigma_{n,k_n}(x, y) = \epsilon\Psi^\sigma_{n,k_n}(x, y). \tag{2}$$

Electrons incident from the two leads ($x \to \pm\infty$) are scattered elastically by the effective QPC potential $\delta V^\sigma(x, y) = V_{\rm QPC}(x, y) + \delta V_H(x, y) + \delta V^\sigma_{\rm xc}(x, y)$, which is the difference between the QPC self-consistent potential and that of the clean wire. The Hartree and exchange-correlation parts of the potentials are written, respectively, as

$$\delta V_H(x, y) = \frac{e^2}{\kappa}\iint dx'dy'\{\rho(x', y') - \rho^0(y')\} \times \left[\frac{1}{\sqrt{(x - x')^2 + (y - y')^2}} - \frac{1}{\sqrt{(x - x')^2 + (y - y')^2 + a^2}}\right], \tag{3}$$

 0031-9007/03/90(2)/026804(4)$20.00

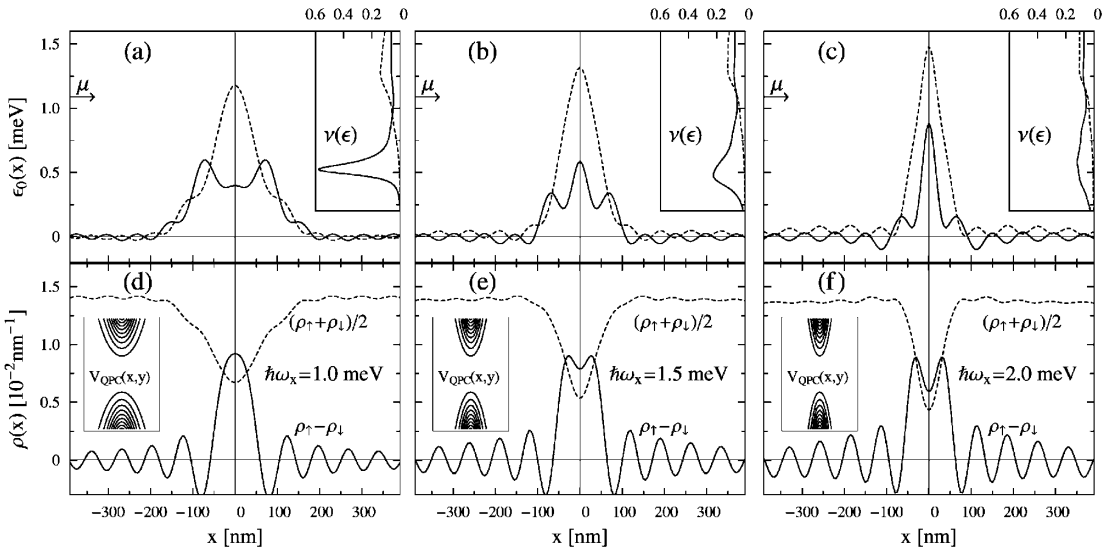

FIG. 1. Results for QPC potentials of increasing sharpness: (a),(d) $\hbar\omega_x = 1.0$ meV, (b),(e) $\hbar\omega_x = 1.5$ meV, and (c),(f) $\hbar\omega_x = 2.0$ meV. (a)–(c) Self-consistent "barrier", i.e., energy of the bottom of the lowest 1D subband $\epsilon_0(x)$ at temperature $T = 0.1$ K as a function of position x in the direction of current flow through QPC. The chemical potential μ is indicated by an arrow on the left. Solid lines are for spin-up and dashed lines are for spin-down electrons. Insets: local density of states $\nu_\sigma(\epsilon)$ at the center of the QPC. (d)–(f) 1D electron density in QPC. The solid line gives the net spin-up density and the dashed line gives the spin-averaged density. Insets: contour plot of the QPC potential $V_{\rm QPC}(x, y)$.

$$\delta V^\sigma_{\rm xc}(x, y) = \frac{\delta E_{\rm xc}[\rho, \xi]}{\delta \rho^\sigma(\mathbf{r})} - \frac{\delta E_{\rm xc}[\rho^0, \xi^0]}{\delta \rho^{0\sigma}(y)}, \qquad (4)$$

where we have introduced an image-charge plane at a distance $a = 100$ nm to model the experimental geometry [18]. The exchange-correlation energy functional $E_{\rm xc}[\rho, \xi]$ is treated in the local-density approximation with the local spin polarization $\xi(\mathbf{r}) = [\rho^\uparrow(\mathbf{r}) - \rho^\downarrow(\mathbf{r})]/\rho(\mathbf{r})$ [20].

The eigenstates of (2) can be characterized as waves incident from the left $\Psi^L_{n,k_n^\sigma}(x, y)$ and from the right $\Psi^R_{n,k_n^\sigma}(x, y)$. Expanding, $\Psi^L_{n,k_n^\sigma}(x, y) = \sum_m u^L_{n,m,k_n^\sigma}(x)\psi^\sigma_m(y)$, $u^L_{n,m,k_n^\sigma}(x)$ has the form of plane waves with wave vectors $k_n^\sigma = \sqrt{2m^*(\epsilon - \epsilon_n^\sigma)}/\hbar$ far from the QPC region:

$$u^L_{n,m,k_n^\sigma}(x) = \begin{cases} e^{ik_n^\sigma x}\delta_{n,m} + r^\sigma_{n,m}e^{-ik_m^\sigma x}; & x \le -x_0, \\ t^\sigma_{n,m}e^{ik_m^\sigma x}; & x \ge x_0, \end{cases} \qquad (5)$$

where $r^\sigma_{n,m}$ and $t^\sigma_{n,m}$ are the elements of unknown reflection and transmission matrices and where $|x_0| = 500$ nm is sufficiently far from the QPC that $\delta V(x, y)$ is negligible. $\Psi^R_{n,k_n^\sigma}(x, y)$ is expanded analogously. We employ the recursion-transfer-matrix method [21] to solve the Kohn-Sham Eq. (2) with the above boundary conditions. From the resulting wave functions, the density $\rho(x, y)$ is constructed as a sum over occupied states,

$$\rho(x, y) = \frac{1}{2\pi}\sum_{\substack{n,\sigma \\ L/R}} \int_0^\infty f\left(\epsilon_n^\sigma + \frac{\hbar^2 k_n^{\sigma 2}}{2m^*}\right)|\Psi^{L/R}_{n,k_n^\sigma}(x, y)|^2 dk_n^\sigma, \quad (6)$$

where the Fermi distribution function is $f(\epsilon) = 1/[\exp\{(\epsilon - \mu)/k_BT\} + 1]$. These procedures are iterated until self-consistent solutions are obtained for the electron density $n_{\rm 1D}$. We use the material constants for GaAs, $m^* = 0.067m_0$, $\kappa = 12.9$, $g = 0.44$ and fix the external confinement in the y direction in the wire such as $\hbar\omega_y = 2.0$ meV.

Figure 1 shows the electronic properties of QPCs with $V_0 = 3.0$ meV at $T = 0.1$ K for three different lengths: (a),(d) $d = 82.6$ nm ($\hbar\omega_x = 1.0$ meV); (b),(e) $d = 55.0$ nm ($\hbar\omega_x = 1.5$ meV); and (c),(f) $d = 41.3$ nm ($\hbar\omega_x = 2.0$ meV). The density far from the QPC is taken as $n_{\rm 1D} = 2.80 \times 10^{-2}\,{\rm nm}^{-1}$, where the electrons far into the wire are unpolarized and only the lowest two spin subbands contribute to transport [18]. We find that a solution with broken spin symmetry coexists with an unpolarized solution. To obtain the broken-symmetry solution, we first apply an in-plane magnetic field of up to $B = 6$ T [14] and then solve the Kohn-Sham equations self-consistently while reducing the magnetic field to zero.

In Figs. 1(a)–1(c) we show the self-consistent QPC barrier as a function of position x in the direction of current flow. Specifically, we plot the energy of the bottom of the lowest 1D subband $\epsilon_0^\sigma(x)$ relative to the band edge ϵ_0^σ far into the wire, for both spin-up (solid lines) and spin-down (dashed lines) electrons. Small Friedel oscillations with a period of $2\pi/2k_f \simeq 72$ nm are present far into the wire. The self-consistent QPC barrier is strongly spin dependent in all three cases, with the chemical potential μ lying above the spin-up barrier but below the spin-down barrier. These observations are consistent with the results of Wang and Berggren [7].

In Figs. 1(d)–1(f) we show the 1D electron density in the QPC. The solid lines give the net spin-up density and the dashed lines give the spin-averaged densities, which

approach $n_{1D}/2 = 1.40 \times 10^{-2}\ \mathrm{nm}^{-1}$ far into the wire. For all three QPC lengths, there is an excess spin-up density in the vicinity of the barrier, with Friedel oscillations persisting into the wire. In each case, the integrated net spin-up density is close to 1 spin: 0.85 for (a), 0.93 for (b), and 0.90 for (c). Thus, there is a local moment with a spin of $1/2$ formed at the QPC.

The local moment found within SDFT results from the self-consistent flattening of the QPC barrier. For example, above a square barrier there is a series of quasibound states, resulting from multiple reflections from the edges of the barrier. While the bare QPC potential does not give rise to resonances, the self-consistent potential is flattened for spin-up, particularly for the longer QPCs, and the first resonance in the spin-up local density of states is clearly resolved. Since this resonance lies below the chemical potential, it is fully occupied. The result is a localized net spin of $1/2$ at the QPC.

An important question is whether SDFT is reliable in predicting a local moment. SDFT is a mean-field theory and has limited utility for strongly correlated electron systems. In particular, consider an Anderson model consisting of a single site with a Coulomb interaction U between two spin-degenerate orbitals of energy ε_0, with hybridization Γ to band electrons [22]. For partially occupied orbitals, the local density of states for each spin splits into two peaks, one at ε_0 and the other at $\varepsilon_0 + U$ (and at low temperatures an additional Kondo peak at the chemical potential) [23]. Taken at face value, SDFT is inadequate for this model as it can give only one peak for each spin. However, SDFT has been applied successfully to calculate local moments in a system closely corresponding to the Anderson model, namely, transition-metal adatoms on surfaces [24]. The key is that, even though the SDFT solution breaks spin-rotation symmetry, the frozen magnetization can still be reliably interpreted as the *magnitude* of the dynamic local moment. In practice, we follow the SDFT method developed by Janak to find the magnetization of metallic metals [25]. Specifically, we first solve the SDFT equations in a polarizing magnetic field and then reduce the field to zero to extract the parameters U and Γ of the underlying Anderson model.

To estimate the properties of the bound state, we go beyond the formal validity of SDFT and study the Kohn-Sham orbitals. Specifically, we plot the local 1D density of states $\nu_\sigma(\epsilon)$ at the center of the QPC in the insets of Figs. 1(a)–1(c) for the respective physical parameters. Below the chemical potential, the local density of states $\nu_\uparrow(\epsilon)$ for spin-up electrons shows a resonance which broadens as the QPC is shortened.

Figure 2 depicts the local 1D density of states $\nu_\sigma(\epsilon)$ for $\hbar\omega_x = 1.5$ meV in the presence of in-plane magnetic fields B from 0 to 10 T in steps of 1 T [14]. Traces are vertically offset by a constant amount. The solid lines are for spin-up and the dashed lines are for spin-down electrons. With increasing Zeeman splitting, the resonance for spin-up electrons shifts to lower energies, while the onset of the spin-down density of states shifts to higher energies. From the residual splitting between these features at $B = 0$, we obtain an estimate for the Coulomb-interaction energy U in a local-moment description of the QPC. Similarly, we obtain the hybridization Γ from the width of the spin-up resonance.

Figure 3 shows the dependence of the Coulomb energy U and the hybridization Γ on the length of the QPC. U is obtained from the energy difference between the resonance center of $\nu_\uparrow(\epsilon)$ and the energy at which the derivative of $\nu_\downarrow(\epsilon)$ is a maximum. Γ is obtained from the FWHM of a Lorentzian fit to the resonance in $\nu_\uparrow(\epsilon)$. The hybridization energy Γ increases sharply from $\Gamma \simeq 0.1$ meV up to $\simeq 0.6$ meV as the QPC is shortened from $d = 80$ nm to $d = 40$ nm. The Coulomb energy U, on the other hand, stays nearly constant at $\simeq 0.6$ meV over this range.

Within the Anderson model, a strong Kondo peak in the differential conductance is expected when $kT < k_B T_K < \Gamma \ll U$. This suggests that there is an optimal range of QPC lengths for observing the Kondo effect: for very long QPCs, Γ and therefore the Kondo temperature T_K will be too small compared to the real temperature, whereas for very short QPCs, the resonance width Γ will be too broad for a Kondo effect ever to develop. Experimentally, Reilly *et al.* [4] observed that the extra conductance plateau in QPCs decreased from $0.7(2e^2/h)$ to $0.5(2e^2/h)$ with increasing QPC length, suggesting a suppression of the Kondo effect [15]. Our SDFT results

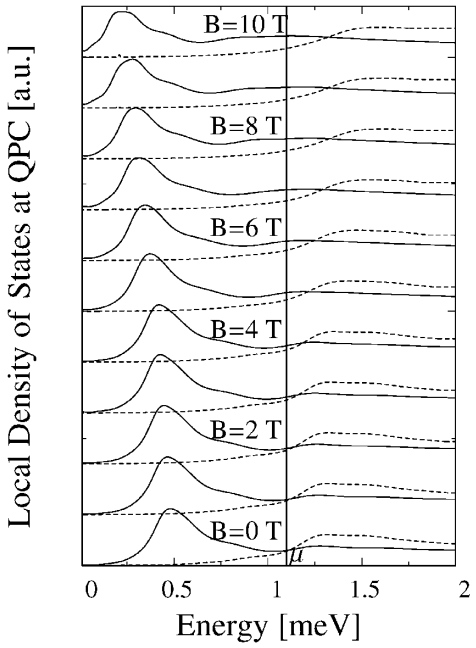

FIG. 2. Local density of states at the center of the QPC for in-plane magnetic fields $B_\parallel$ from 0 to 10 T in steps of 1 T [14]. Traces are vertically offset by a constant amount. The solid lines are for spin-up and the dashed lines are for spin-down electrons.

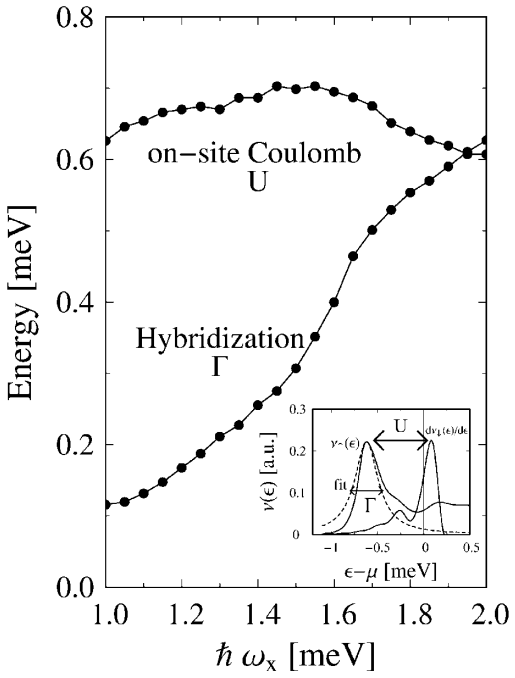

FIG. 3. Hybridization energy Γ and on-site Coulomb energy U as a function of $\hbar\omega_x$, the sharpness of the external QPC potential. Γ is obtained from the FWHM of the Lorentzian fit to the resonance. U is obtained from the energy difference between the resonance center and the maximum of $d\nu(\epsilon)/d\epsilon$ for the high-energy spin. Inset: $\nu_\uparrow(\epsilon)$ and $d\nu_\downarrow(\epsilon)/d\epsilon$ at the center of QPC for $\hbar\omega_x = 1.5$ meV. The dashed line is the Lorentzian fit to the resonance of $\nu_\uparrow(\epsilon)$. Hybridization energy Γ and on-site Coulomb energy U are indicated.

suggest that it is primarily the decreasing hybridization of the local moment to the leads that is responsible for the decrease of the Kondo temperature and the evolution of the conductance plateau.

We have presented SDFT results only for chemical potentials sufficiently above the resonance energy that the local moment is fully formed. SDFT is generally unreliable for a partially filled orbital, unless self-interaction effects are explicitly removed [26], and this is not practical for an open system with long range interactions such as a QPC.

In conclusion, we studied the electronic states of quantum point contacts using the spin-density-functional method. We found that a local moment with a spin of $1/2$ is formed in the vicinity of the QPC barrier. This strongly supports recent claims of a Kondo effect in transport through a quantum point contact [13]. For the local moment, we obtained estimates for both the on site Coulomb-interaction energy and the hybridization to the leads. The latter decreases rapidly with increasing length of the QPC.

The work by Y. M. at Rutgers was partially supported by NSF Grant No. DMR 00-93079 and by DOE Grant No. DE-FG02-00ER45790, and K. H. acknowledges useful discussions with Shu-Shen Li.

Note added.—Recently, K.-F. Berggren and I. I. Yakimenko reported evidence for ferromagnetism in a QPC based on spin-density functional calculations [27]. The net ferromagnetism was less than one electron spin, consistent with our interpretation of local-moment formation at the QPC.

*Permanent Address: Department of Physics, Ben-Gurion University, Beer Sheva 84105, Israel.

[1] K. J. Thomas *et al.*, Phys. Rev. Lett. **77**, 135 (1996); K. J. Thomas *et al.*, Phys. Rev. B **58**, 4846 (1998).
[2] A. Kristensen *et al.*, Phys. Rev. B **62**, 10 950 (2000).
[3] S. Nuttinck *et al.*, Jpn. J. Appl. Phys. **39**, L655 (2000); K. Hashimoto *et al.*, *ibid.* **40**, 3000 (2001).
[4] D. J. Reilly *et al.*, Phys. Rev. B **63**, 121311 (2001).
[5] B. J. van Wees *et al.*, Phys. Rev. Lett. **60**, 848 (1988).
[6] D. A. Wharam *et al.*, J. Phys. C **21**, L209 (1988).
[7] C.-K. Wang and K.-F. Berggren, Phys. Rev. B **57**, 4552 (1998).
[8] V.V. Flambaum and M.Y. Kuchiev, Phys. Rev. B **61**, R7869 (2000).
[9] B. Spivak and F. Zhou, Phys. Rev. B **61**, 16 730 (2000).
[10] T. Rejec and A. Ramsak, Phys. Rev. B **62**, 12 985 (2000).
[11] H. Bruus, V.V. Cheianov, and K. Frensberg, Physica (Amsterdam) **10E**, 97 (2001).
[12] Y. Tokura and A. Khaetskii, Physica (Amsterdam) **12E**, 711 (2002).
[13] S. M. Cronenwett *et al.*, Phys. Rev. Lett. **88**, 226805 (2002).
[14] A magnetic field in the plane of the QPC induces a Zeeman splitting between spin-up and spin-down electrons without affecting their orbital degrees of freedom.
[15] Y. Meir, K. Hirose, and N. S. Wingreen, Phys. Rev. Lett. **89**, 196802 (2002).
[16] E. Lieb and D. Mattis, Phys. Rev. **125**, 164 (1962).
[17] J. Callaway and N. H. March, Solid State Phys. **38**, 135 (1984).
[18] K. Hirose, S. S. Li, and N. S. Wingreen, Phys. Rev. B **63**, 033315 (2001); K. Hirose and N. S. Wingreen, *ibid.* **64**, 073305 (2001).
[19] W. Kohn and L. J. Sham, Phys. Rev. **140**, A1133 (1965).
[20] We use the parametrized form by B. Tanatar and D. M. Ceperley [Phys. Rev. B **39**, 5005 (1989)] for the two-dimensional electron gas for the local exchange-correlation energy.
[21] K. Hirose and M. Tsukada, Phys. Rev. B **51**, 5278 (1995).
[22] P.W. Anderson, Phys. Rev. **124**, 41 (1961).
[23] A. C. Hewson, *The Kondo Problem to Heavy Fermions* (Cambridge University, Cambridge, 1997).
[24] V. S. Stepanyuk *et al.*, Phys. Rev. B **53**, 2121 (1996).
[25] J. F. Janak, Phys. Rev. B **16**, 255 (1977).
[26] J. P. Perdew and A. Zunger, Phys. Rev. B **23**, 5048 (1981).
[27] K.-F. Berggren and I. I. Yakimenko, Phys. Rev. B **66**, 085323 (2002).